ARTICLE IN PRESS

Available online at www.sciencedirect.com

SCIENCE DIRECT®

Biomaterials ▮ (▮▮▮▮) ▮▮▮–▮▮▮

Biomaterials

www.elsevier.com/locate/biomaterials

Processing and properties of porous poly(L-lactide)/bioactive glass composites

Kai Zhang[a,1], Yunbing Wang[b,2], Marc A. Hillmyer[b], Lorraine F. Francis[a,*]

[a] *Department of Chemical Engineering and Materials Science, University of Minnesota, 421 Washington Avenue SE, Minneapolis, MN 55455-0132, USA*

[b] *Department of Chemistry, University of Minnesota, 207 Pleasant Street SE, Minneapolis, MN55455, USA*

Received 7 April 2003; accepted 4 September 2003

Abstract

Porous poly(L-lactide)/bioactive glass (PLLA/BG) composites were prepared by phase separation of polymer solutions containing bioactive glass particles (average particle size: 1.5 μm). The composite microstructures consist of a porous PLLA matrix with glass particles distributed homogeneously throughout. Large pores (>100 μm) are present in a network of smaller (<10 μm) interconnected pores. The porous microstructure of the composites was not significantly influenced by glass content (9 or 29 vol%), but silane pretreatment of the glass resulted in better glass incorporation in the matrix. Mechanical tests showed that an increase in glass content increased the elastic modulus of the composites, but decreased their tensile strength and break strain. Silane pretreatment enhanced the increase in modulus and prevented the decrease in tensile strength with increasing glass content. Composites soaked in simulated body fluid (SBF) at body temperature formed bone-like apatite inside and on their surfaces. The silane pretreatment of glass particles delayed the in vitro apatite formation. This bone-like apatite formation demonstrates the composites' potential for integration with bone.

Keywords: Porosity; Polylactic acid (PLA); Bioactive glass; Composite; Silane; Apatite

1. Introduction

Porous polymer/ceramic composites [1–15] are of interest for guided tissue regeneration (GTR) membranes [5,6], and bone tissue engineering scaffolds [1–4,7–11,13–15]. In vitro and in vivo tests demonstrate that porous composites can serve as matrices for bone cell growth and differentiation [7,8,15], and show that composites have better osteoconductivity compared with porous polymers alone [7].

Another promising application for porous composites is at the interfaces between soft and hard tissues [12,16–22]. The problem of anchoring cell culture-derived artificial soft tissues (e.g., cartilage) to host hard tissue (bone) [12,17,20] may be solved by constructing an interface composite; one side of the composite serves as a substrate to grow artificial soft tissue and the other subsequently attaches to native bone [12]. The composites should be compatible with both soft and hard tissues and be porous for tissue mechanical interlocking and body fluid transfer [12].

Porous composites have been prepared by salt-leaching [3,8,15], thermally induced phase separation (TIPS) [7,13], dry phase inversion [6], sintering of microspheres containing polymer and ceramic fillers [1,4], solid freeform fabrication (SFF) [23], in situ polymerization in porous ceramics [11], and mineralization of porous polymer scaffolds by biomimetic methods [2,9,14]. Meanwhile, new components, processing techniques and applications for the porous polymer/ceramic composites are still an important topic for further studies [24,25].

Many of the porous composites studied to-date are composed of a biodegradable polymer (e.g., polylactide) and a bioceramic phase (e.g., synthetic hydroxyapatite)

*Corresponding author. Tel.: +1-612-625-0559; fax: +1-612-626-7246.

E-mail address: lfrancis@umn.edu (L.F. Francis).

[1] Biomaterials group, Polymers division, National Institute of Standards and Technology (NIST), Gaithersburg, MD 20899.

[2] Medtronic MiniMed Inc., 18000 Devonshire St., Northridge, CA, 91325.

0142-9612/$ - see front matter © 2003 Elsevier Ltd. All rights reserved.
doi:10.1016/j.biomaterials.2003.09.033

[1–10,13–15]. A candidate for the bioceramic phase in porous composites is bioactive glass (BG). Bioactive glass bonds chemically to both hard and soft tissues by development of a biologically active apatite layer [26]. The incorporation of bioactive glass in the porous composite encourages bonding to bone and may influence calcification in the artificial soft tissue [27]. Dense composites containing biodegradable [5,28] or non-biodegradable [29,30] polymers and bioactive glass fillers have been developed. More recently, porous polymer/bioactive glass composites have received attention [5,10,12,16,31,32]. Although the mechanical properties of porous composites are a concern due to the porous structure and the potentially weak interface between polymer and ceramic phase [12,33], mechanical properties can be improved by modification of the polymer phase and/or ceramic phase [33,34].

In this study, a phase separation technique [12,16,35] is used to process porous poly(L-lactide)/bioactive glass (PLLA/BG) composites. The effects of bioactive glass content and pretreatment of the glass with 3-aminopropyltrimethoxylsilane (APS) on the microstructure, mechanical properties and apatite formation behavior of the composites were studied. The potential bone integration ability of the porous PLLA/BG composites is demonstrated in an in vitro model of simulated body fluid (SBF).

2. Materials and methods

2.1. Materials

PLLA (containing 98 mol% L-isomer) used in this study was generously provided by Cargill-Dow Polymer, LLC [36] and purified in our laboratory by dissolution in chloroform (5% w/v) followed by precipitation into a fivefold volume of methanol. Thermal analysis by a differential scanning calorimetry (DSC, Perkin-Elmer DSC-7) showed that the PLLA has a melting point of 169°C. The size exclusion chromatography analysis gave a number average molecular weight (M_n) of 83.1 kg/mol and a polydispersity index (M_w/M_n) of 1.67.

Bioactive glass with an average particle size of 6.8 μm (as measured by a Coulter® LS 230 Particle Analyzer) and a composition of 4.6MgO, 44.7CaO, 34.0SiO_2, 16.2 P_2O_5 and 0.5 CaF_2 (wt%) was purchased from Specialty Glass, Inc. The bioactive glass was further processed in an attrition mill to achieve an average particle size of 1.5 μm (as measured by a Coulter® LS 230 Particle Analyzer) and a BET surface area of 4.95 m^2/g (as-measured by a Gas Sorptometer, Micromeritics model ASAP 2000).

3-aminopropyltrimethoxysilane (APS), 1,4-dioxane, reagent-grade chemicals NaCl, $NaHCO_3$, KCl, $K_2HPO_4 \cdot 3H_2O$, $MgCl_2 \cdot 6H_2O$, $CaCl_2$ and trishydroxymethyl aminomethane (Tris buffer, $(CH_2OH)_3CNH_2$) were purchased from Aldrich, Inc.

2.2. Pretreatment of bioactive glass particles by APS

Some as-milled glass particles were pretreated with 3-aminopropyltrimethoxysilane (APS). APS has the ability to bond to both polylactide and bioceramic particles [37]. A hydrolyzed APS solution was prepared by adding APS (1 wt%) to a solution composed of 95 wt% ethanol and 5 wt% water and mixing for 30 min. As-milled bioactive glass particles were dispersed in the hydrolyzed APS solution. After 2 h, the glass suspension was centrifuged and filtered. Glass particles were then dried under vacuum at 25°C overnight. The amount of APS required for silanization was estimated by the following equation [38]:

$$X = (A/w)f, \quad (1)$$

where X is the amount of APS needed for a minimum uniform coverage of glass particles (g), A is the glass surface area (4.95 m^2/g), w is the wetting surface of APS (353 m^2/g, adapted from the value of 3-aminopropyltriethoxylsilane reported by the Petrarch Systems Inc.), and f is the amount of glass particles (g). Three times the estimated amount of APS was used for the pretreatment of the glass particles [38].

A thermogravimetric analyzer (Perkin-Elmer TGA-7) was used to characterize the APS pretreated glass particles and control (non-treated) glass particles. Weight loss was measured as the specimens were heated from 35°C to 800°C. A Nicolet Magna-IR 750 (diffuse reflectance mode, DRIFTS) spectrometer was used to investigate the surface structure change of glass particles before and after APS treatment.

2.3. Preparation of porous PLLA/bioactive glass (PLLA/BG) composites

Porous PLLA/BG composites were prepared by a phase separation technique based on a method designed for polylactide membranes [39] that was adapted to include bioactive glass particles [12,16]. Homogeneous dispersions were made by adding bioactive glass particles to a mixture of 1,4-dioxane (8.37 g, a solvent for PLLA) and water (0.63 g, a non-solvent for PLLA), and then dissolving PLLA (1 g) into the glass dispersion. Dispersions with different glass contents (with and without APS treatment) were prepared. See Table 1. TGA results confirmed the weight ratios of PLLA to BG in Table 1. Dispersions were cast onto glass substrates by a doctor blade (gap height = 800 μm). The resulting coated substrates were immediately immersed in a water bath and held there for at least 10 min for phase separation. The composite coatings separated from t heir substrates in the water bath. The free-standing

composites were dried at room temperature for at least 24 h before further analysis. Porous PLLA specimens (with no BG particles) were also prepared using this method.

2.4. Characterization of porosity and mechanical properties

The porosity of composites was determined from bulk density measurements, using 1.26 g/cm^3 for density of PLLA and 3.0 g/cm^3 for bioactive glass. Data reported in Table 1 show the average data from 5 specimens.

The mechanical tests of porous PLLA and composites (with and without APS pretreatment of glass particles; dimensions: ~30 mm (length) by ~3 mm (width)) were performed with a dynamic mechanical analyzer (Perkin-Elmer DMA-7) attached to a PC via a DMA7/DX thermal controller. A static stress mode (loading rate: 500 mN/min) was used for tensile tests. Elastic modulus was calculated from the elastic region of the stress-strain curve (up to 0.5% strain for 29BG, 1.0% strain was used for all other samples). Tensile strength and break strain were also determined. Results are reported for data collected from at least 5 specimens for each material (see Table 2). Statistical analysis of the data was performed using a student's t test with a level of significance of $p<0.05$.

2.5. Model for composites' elastic modulus

The effects of glass and pore content on the elastic modulus of porous composites are accounted for in a model described in detail elsewhere [12]. The total glass volume fraction (V_T) is the sum of the glass fraction incorporated in the matrix (V_{G1}) and that in the pore space (V_{G2}). The elastic modulus of the porous composite (E) is given by:

$$E = E_0[1-(P+V_{G2})]^n, \quad (2)$$

where E_0 is the modulus of the solid composite matrix (without pores), P is the pore fraction and n is a constant that depends on the microstructure [40]. When the experimental data for E and P of porous poly (L-lactide) (PLLA) ($V_{G2}=0$) are inserted into Eq. (2) along with the reported modulus of dense polylactide (2560 MPa) [41], the constant n is found to be 1.97. This value is close to 2, the theoretically predicted value for open cell foams [40]. For the composites in this study, E_0 depends on the amount of glass incorporated into the polymer matrix, relative to the solid volume. The following expression was adapted from a model developed by Ishai and Cohen [42]:

$$E_0 = E_P\left(1+\frac{[V_{G1}/1-(P+V_{G2})]}{m/(m-1)-[V_{G1}/1-(P+V_{G2})]^{1/3}}\right), \quad (3)$$

where E_P is the modulus of the polymer, and m is the ratio of the modulus of the glass to that of the polymer. By combining Eqs. (2) and (3) and assuming $E_P = 2560$ MPa, $n = 1.97$, $m = 34.8$ (the modulus of the glass is 89 GPa [43]), V_{G1}, V_{G2} and E_0 can be predicted for each composite (see Table 3).

2.6. Study of bone-like apatite growth in simulated body fluid (SBF)

Simulated body fluid (SBF) was prepared according to Kokubo et al. [44]. Composites (~1 × 1 cm) were

Table 1
Composition and porosity of porous PLLA and PLLA/BG composites

Specimen	Glass particle pretreatment	PLLA:BG (wt. ratio)	Glass vol% in composite[a]	Average porosity (%)[b]
PLLA	No	0	0	80
9BG	No	4:1	9.4	77
29BG	No	1:1	29.2	78
9BG/S	Yes	4:1	9.4	80
29BG/S	Yes	1:1	29.2	79

[a] Relative to total solids.
[b] Determined by bulk density method.

Table 3
Predictions of glass incorporated[a] into the polymer matrix and matrix modulus

Specimen	V_T	P[b]	E[c] (MPa)	V_{G1}	V_{G2}	E_0 (MPa)
9BG	0.022	0.77	145.08	0.014	0.008	2813.8
29BG	0.064	0.78	178.59	0.049	0.015	4052.3
9BG/S	0.019	0.80	136.74	0.019	0	3257.4
29BG/S	0.061	0.79	259.64	0.061	0	5618.2

(using $E = 2560$ MPa, $n = 1.97$).
[a] See text for definitions.
[b] Determined from bulk density measurements of composites.
[c] Average from DMA analysis.

Table 2
Mechanical properties of porous PLLA and PLLA/BG composites

Mechanical properties	PLLA	9BG	29BG	9BG/S	29BG/S
Elastic modulus (MPa)	107.7±16.3	145.1±8.6	178.6±14.4	136.7±15.9	259.6±43.2
Tensile strength (MPa)	3.2±0.4	2.6±0.2	1.5±0.3	3.9±0.4	3.0±0.7
Break stain (%)	8.7±2.5	2.7±0.5	1.1±0.2	13.7±3.8	1.8±0.4

soaked individually in 50 ml SBF at 37°C. The soaked composites were transferred to SBF immediately after the phase separation was complete in the water bath. The SBF was changed every other day. After 1 and 2 week time points, composites were removed, washed with ethanol and then dried at room temperature for further characterization. Porous PLLA specimens were also soaked and prepared by the same procedure.

2.7. Microstructure characterization

Porous PLLA and PLLA/BG composites before and after soaking in SBF were characterized by scanning electron microscopy (SEM, Hitachi S800). SEM specimens were prepared by freezing fracture of samples in liquid nitrogen and then sputter coating with 50 Å platinum. X-ray diffraction (XRD) and FTIR spectroscopy data were also collected using a Bruker-AXS microdiffractometer with 2.2 kW sealed Cu X-ray source and a Nicolet Magna-IR 750 (diffuse reflectance mode, DRIFTS) spectrometer, respectively.

3. Results

3.1. Microstructure of porous PLLA/BG composites

SEM images of composite 9BG are shown in Fig. 1. The average thickness of the composite is ~300 μm. The structure consists of a dense skin layer (Fig. 1D) on the surface that was in contact with the water bath, and a porous supporting layer with small and large pores (Fig. 1A and 1B). The size of the larger pores is between 50 and 200μm; the average size of the smaller pores is less than 10μm. The bottom surface (Fig. 1C) is also porous with an average pore size of 20μm. This porous structure is a characteristic morphology of the polylactide membranes formed by the phase separation method [39]. The glass particles (see Fig. 1B) are well distributed throughout the composite; they appear on the pore surfaces, and in the polymer matrix.

The effect of changing bioactive glass content on the microstructure relative to composite 9BG (Fig. 1) is shown in Fig. 2. The microstructures of porous PLLA (Fig. 2A and B) and composite 29BG (Fig. 2C and D)

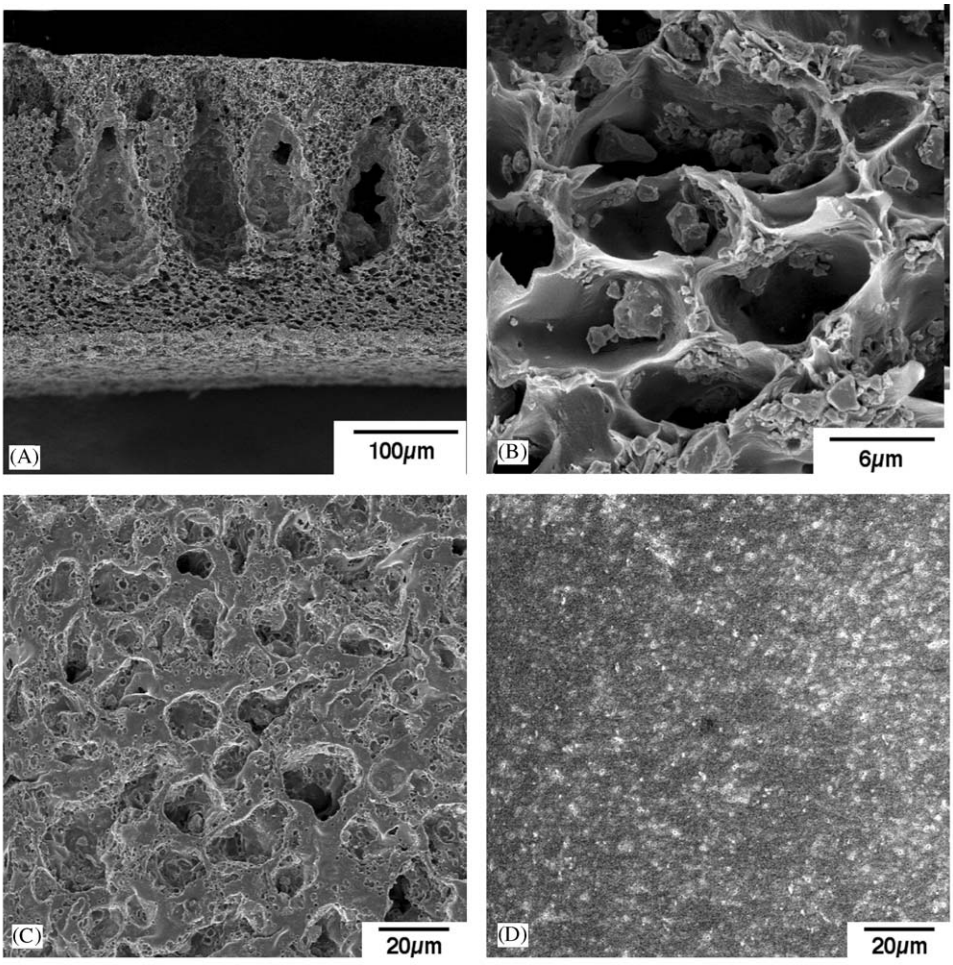

Fig. 1. SEM images of composite 9BG. (A) cross-section and (B) cross-section (high magnification), (C) bottom surface, and (D) top surface.

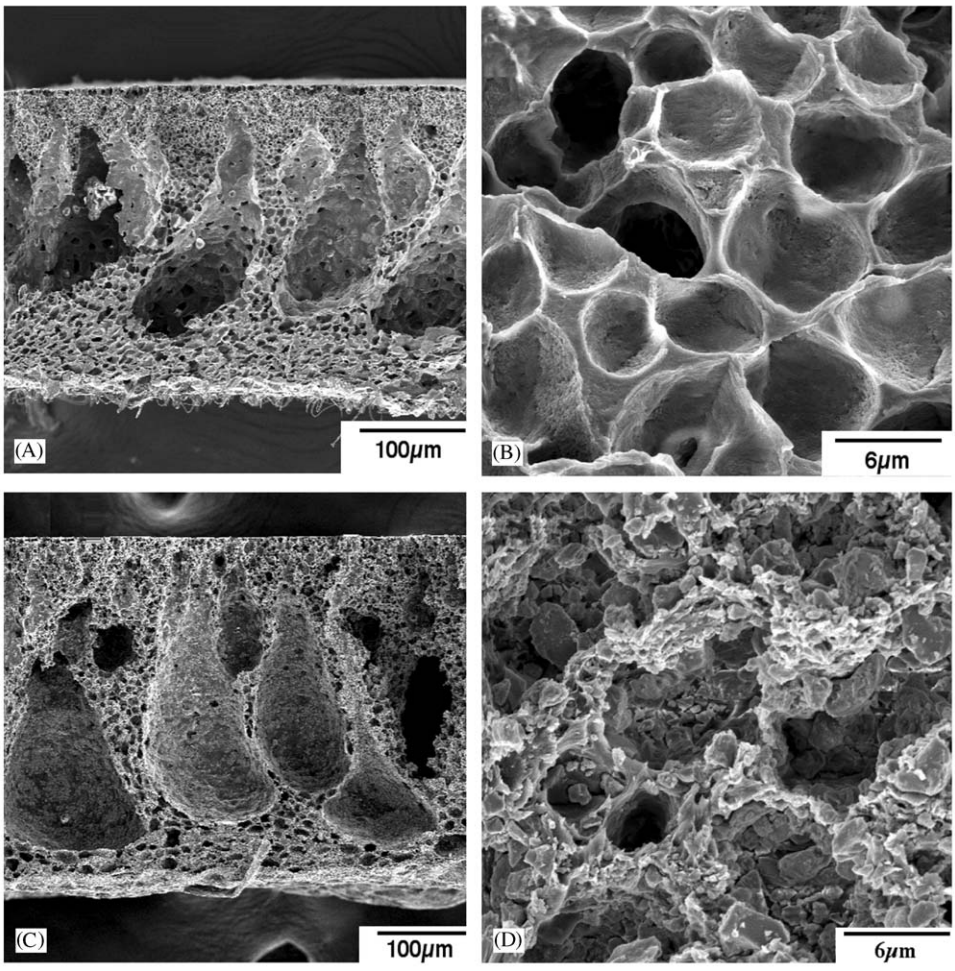

Fig. 2. Cross-section SEM images of (A) PLLA, (B) PLLA (high magnification), (C) composite 29BG, and (D) 29BG (high magnification).

contain the features described above and are similar to those of 9BG. Increasing the glass content from 9 Vol% (9BG) to 29 Vol% (29BG) did not alter of the porous structure much, but more glass particles appear on the pore surfaces (Fig. 2D).

The effects of APS pretreatment of bioactive glass particles on the microstructure of porous composites are shown in Fig. 3. Compared with the composites containing the same amount of non-treated glass (Figs. 1B and 2D), composites containing pretreated glass have a similar porous structure, but with fewer glass particles exposed on the pore surfaces (Fig. 3B and D). The pretreatment appeared to facilitate glass incorporation in the PLLA matrix.

Fig. 4 shows the FTIR-DRIFTS spectra for bioactive glass particles before and after APS modification. The difference spectrum (Fig. 4 inset) has bands at 1587 and 2932 cm^{-1}. These locations are consistent with the NH_2 group (deformation mode) and C–H bond (stretching mode) [45] from APS adsorbed on the glass surface.

Fig. 5 shows the TGA data for bioactive glass particles (non-treated) and bioactive glass particles with APS pretreatment. The higher weight loss after 280°C for the pretreated particles is due to the loss of APS from glass surface. Using the weight loss data, the amount of adsorbed APS is 0.26 wt% (relative to the glass weight). Only a fraction of the APS added to the suspension (4.2 wt%, see Materials and Methods) adsorbed on the glass surfaces, the remainder was removed in the supernatant after centrifugation. However, the adsorbed APS has dramatic effects on the microstructure and mechanical properties of porous composites.

3.2. Mechanical properties

Representative stress-strain curves for porous PLLA and PLLA/BG composites are shown in Fig. 6. Table 2 gives all mechanical properties data. For composites prepared with non-treated bioactive glass particles, the elastic modulus of the composites increases with the

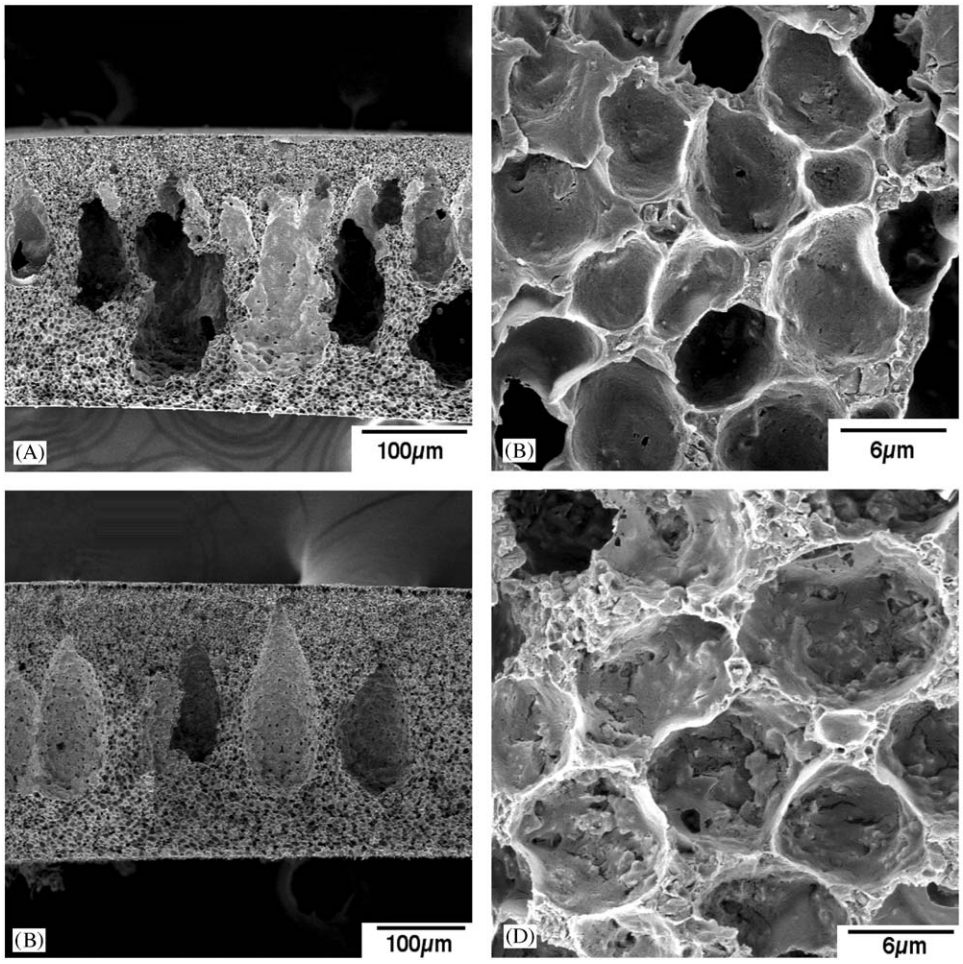

Fig. 3. Cross-section SEM images of composites containing APS-pretreated glass particles. (A) 9BG/S, (B) 9BG/S, cross-section (high magnification), (C) 29BG/S, and (D) 29BG/S (high magnification).

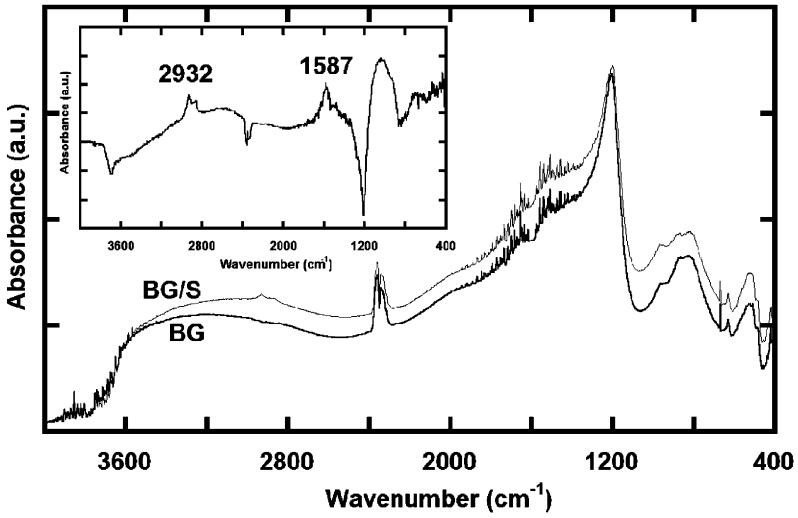

Fig. 4. FTIR spectra of bioactive glass particles before (BG) and after (BG/S) APS modification, and the difference spectrum (inset) obtained by digitally subtracting the absorbance contribution of BG from the spectrum of BG/S.

addition of bioactive glass particles, but the tensile strength and break strain decrease significantly. The addition of silane pretreated glass particles also increases the elastic modulus of the composites, but in this case, the tensile strength does not decrease. Compared with the strength of porous PLLA, the strength of 9BG/

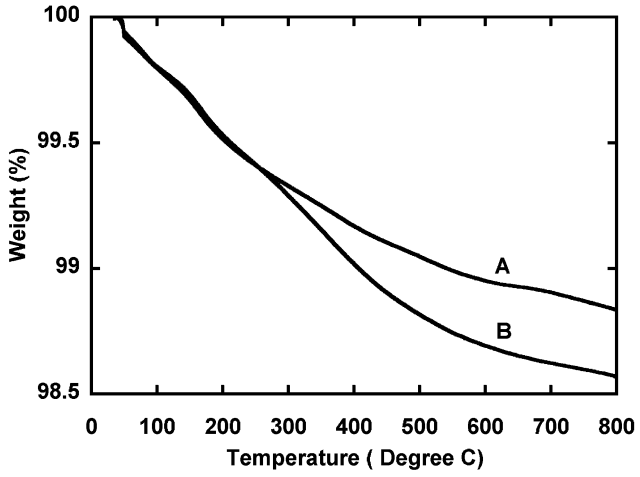

Fig. 5. TGA data for bioactive glass particles before (BG) and after (BG/S) APS pretreatment.

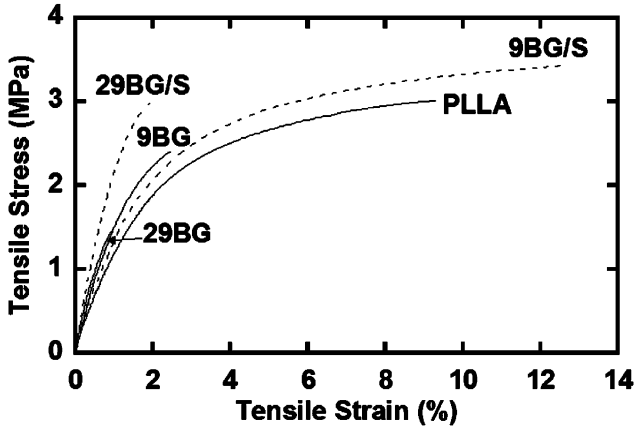

Fig. 6. Typical tensile stress-strain curves for the porous samples listed in Table 2.

S is higher and that of 29 BG/S is the same (no statistical difference). The break strain of the composites with the smaller amount of pretreated glass (9BG/S) is not statistically different from that of the porous PLLA. However, when more pretreated glass particles were added (29BG/S), the break strain of the composites is statistically lower than that of the porous PLLA.

Comparing the composites with the same glass content (9BG vs. 9BG/S; 29BG vs. 29BG/S), the composites containing silane pretreated glass have statistically significant higher break strain and tensile strength. Although the elastic modulus of 9BG/S is not statistically different from that of 9BG, the elastic modulus of 29BG/S is higher than that of 29BG. The effects of addition of glass and silane pretreatment on the elastic modulus can also be observed from the predicted values of elastic modulus of the porous composites' matrix (E_0) (see Table 3). E_0 was enhanced by the increased amount of glass incorporated in the polymer.

3.3. Bone-like apatite growth

Fig. 7 shows the SEM images of 9BG after soaking in SBF for 1 week. Compared to before soaking (see Fig. 1), the surface and interior structures of the composites are different. New, flake-like material is found on the surface and inside the composites after soaking. Both the bottom (Fig. 7B) and top surfaces (Fig. 7C) developed a continuous layer of new material composed of micron-sized clusters with a fine texture. In comparison to 9BG, no flake-like materials formed on either PLLA or composite 29BG after 1 week soaking in SBF.

Fig. 8 shows the XRD patterns of the 9BG composite before and after soaking in the SBF. The composite bottom surface was analyzed. Before soaking, only the peaks of PLLA appeared. After soaking 1 week in the SBF, broad apatite peaks (JCPDS 9-0432) were observed, showing that the new material observed on the composites is crystalline bone-like apatite. The FTIR-DRIFTS spectra (not shown) contained characteristic bands for phosphate and carbonate groups [46], also indicating that the new material is apatite.

Fig. 9 shows the SEM images of PLLA and the 29BG composite after soaking in SBF for 2 weeks. While a few apatite clusters formed on the top surface of the PLLA, no apatite formed inside the porous PLLA (Fig. 9A). The microstructure of the 29BG composite after soaking 2 weeks is shown in Fig. 9B. Apatite developed on the surfaces and inside the composites. This result was also confirmed by XRD. No apparent apatite morphology difference inside the composite 9BG was observed between 1 and 2 weeks of soaking in SBF.

The effect of silane pretreatment of bioactive glass on the apatite development for porous composites was also studied. Fig. 10 shows the microstructure of the composite 9BG/S after soaking in SBF for 1 and 2 weeks. After one week, spherical clusters, which may be precursors for apatite, appeared both inside and on the surfaces of the composites. After 2 weeks, apatite clusters with a size between several hundred nanometers to one micron are found.

4. Discussion

4.1. Microstructure of porous PLLA/BG composites

Porous PLLA/BG composites were created by a phase separation method. The microstructures are similar to those of other porous polymer/ceramic composites formed by this method [12,16]. The most striking observation for these microstructures is the effect of silane pretreatment on glass incorporation. SEM observations (see Fig. 3) and mechanical properties modeling results (see Table 3) show this enhanced incorporation. The interaction can be understood in

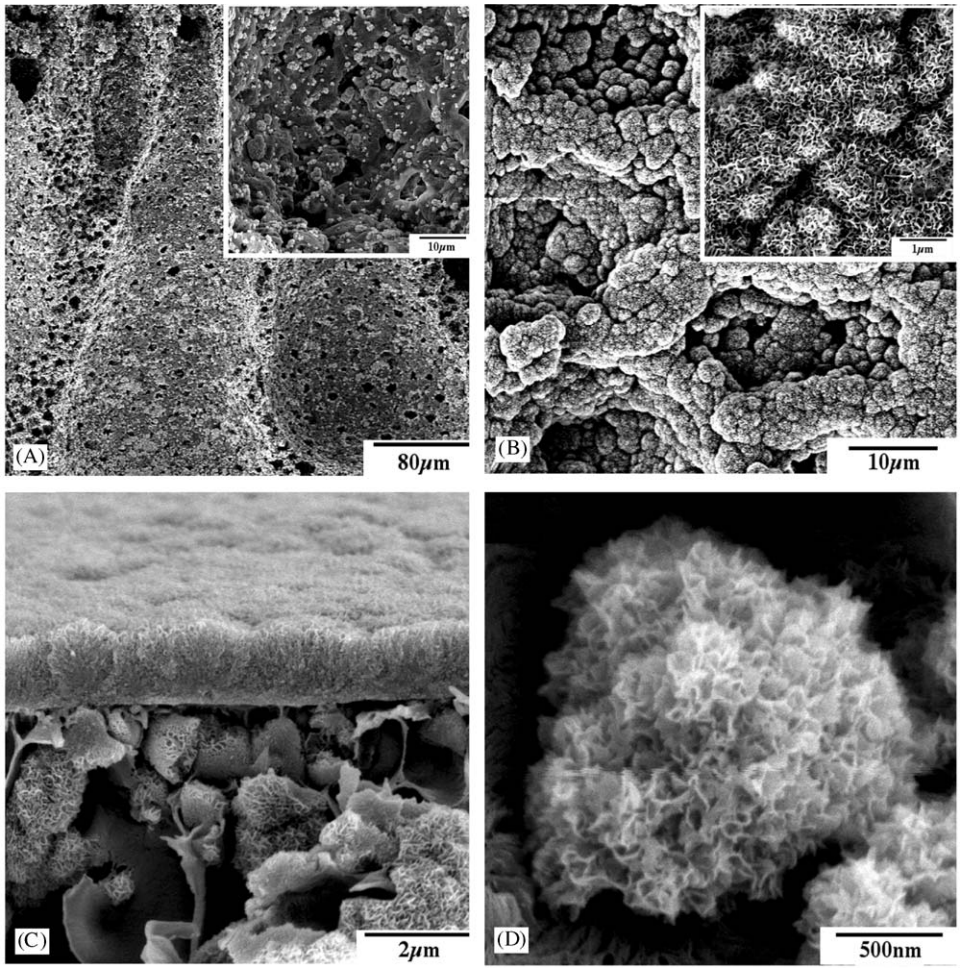

Fig. 7. SEM images of 9BG after soaking in SBF for 1 week: (A) cross-section (inset shows high magnification), (B) bottom surface (inset shows high magnification), (C) top and cross-section, and (D) cross-section (high magnification).

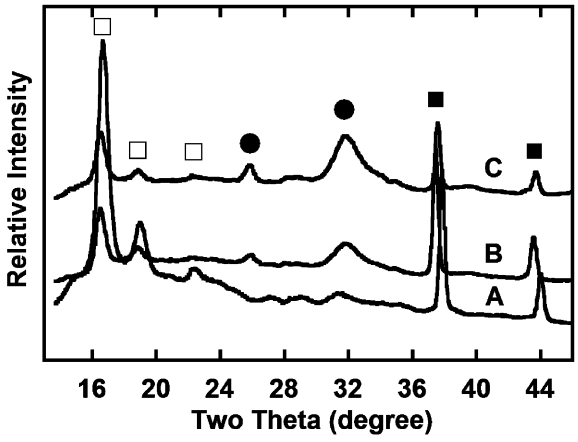

Fig. 8. XRD patterns for 9BG (A), 9BG after soaking in SBF for 1 week (B) and 9BG after soaking in SBF for 2 weeks (C). Peaks for apatite, PLLA and the Al holder are shown by solid spheres, empty squares, and solid squares, respectively.

terms of the chemistry of silane, the glass surface, and PLLA [47]. APS hydrolyses during processing, and the resultant silanol groups can bond with the glass particle surface. Amine groups from APS can form hydrogen bonds to COO–sites on the hydrolyzed PLLA backbone. Silane treated glass particles are better incorporated into polymer-rich phase during the phase separation process. Therefore, an improved interface between PLLA and glass particles is formed with the coverage of PLLA on glass particles.

The porous structure of these composites is suitable for several applications. As one of the potential applications is for the interface connecting artificial soft tissue to host hard tissue, developing porous surface structure is also desired. Surface pores may be encouraged by incorporation solvent in the coagulation solution [48], by adding an abrasion step [12], or by combining phase separation with a salt leaching technique [16].

4.2. Mechanical properties

The elastic modulus of porous polymer/bioactive glass composites is affected by both the porosity of composites and the glass particles incorporated in the

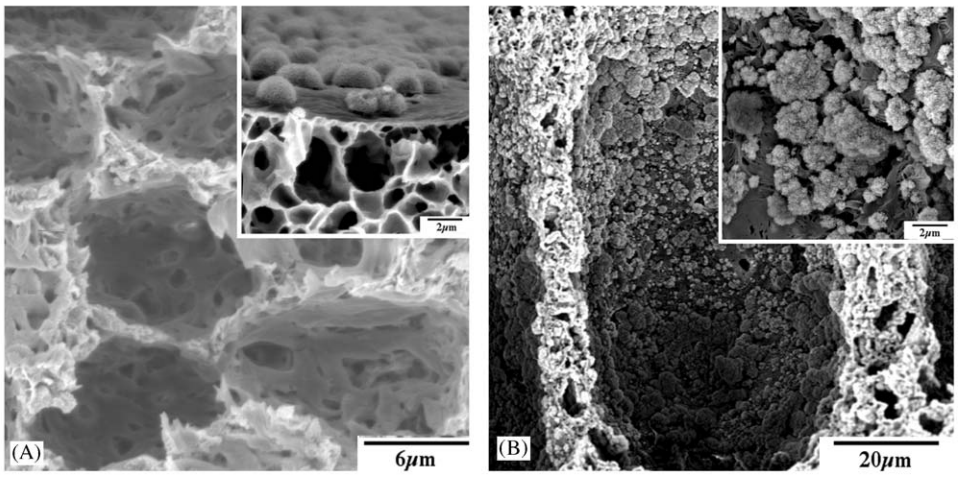

Fig. 9. SEM images of cross-sections of (A) PLLA after soaking in SBF for 2 weeks; inset shows higher magnification and reveals surface and (B) 29BG after soaking in SBF for 2 weeks. Inset shows higher magnification.

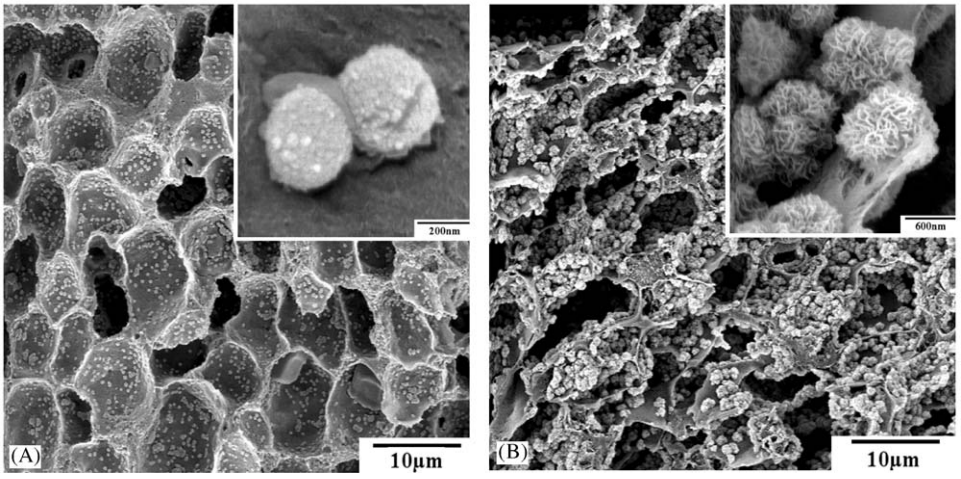

Fig. 10. SEM images of the cross-sections of (A) 9BG/S after soaking in SBF for 1 week and (B) 9BG/S after soaking in SBF for 2 weeks. Insets show higher magnification.

polymer matrix [12]. Using a model developed previously [12], the two effects can be decoupled, and the effects of glass content and silane pretreatment revealed. The predicted elastic modulus of the solid matrix (E_0) and the measured modulus of the composite (E) increase with glass content for porous composites with treated or untreated BG (see Table 3). The effect of APS pretreatment on the elastic modulus of composites can be observed by comparing 9BG with 9BG/S, and 29BG with 29BG/S. In both cases, E_0 is higher for the composite containing silane treated glass. Here, the model also reveals the enhanced incorporation of glass into the polymer matrix; V_{G1} (the fraction of the glass incorporated in the matrix) is higher for composites prepared with silane treated glass. This finding is consistent with the SEM observations (see Fig. 3). The comparison of measured moduli shows the effect of the small variations in pore content. The measured moduli of 9BG/S and 9BG are not statistically different, because 9BG/S has a higher pore content, which counters the effect of greater glass incorporation in the matrix. The measured modulus of 29BG/S is significantly higher than that of 29BG; the pore contents are nearly the same in this case.

Silane treatment of BG particles also improved the tensile strength of porous PLLA/BG composites. The enhanced strength can be attributed to the increased incorporation of BG particles in the PLLA matrix and improved bonding at the interface between them [49–51]. However, silane pretreatment does not prevent the decrease in ductility that occurs at the higher BG content (29BG/S). Increasing the amount of non-deformable glass eventually lowers the strain to failure of the composite.

4.3. Bone-like apatite growth

Formation of apatite in and on porous polymer/bioactive glass composites depends on several factors: the polymer's native ability to form apatite in SBF [14], incorporation of bioactive glass [12], and the relative surface area and amount of bioactive glass (or polymer) compared to the volume of SBF [52]. Porous PLLA scaffolds can develop bone-like apatite after soaking in SBF [14]. The apatite formation mechanism for porous PLLA [14] is related to the hydrolysis of PLLA, which results in a negatively charged PLLA surface. The positively charged calcium ions in the solution are attracted to the hydrolyzed PLLA surface and apatite forms through the attraction of phosphate groups from the solution and the increase of local apatite ion activity product [14]. In this research, the apatite formation ability of porous PLLA is demonstrated by the apatite development on the PLLA outer surfaces after 2 weeks soaking in SBF (see Fig. 9A). This apatite formation timeframe is similar to that reported in other studies [14]. The fact that apatite grows only on the outer surface of porous PLLA is consistent with the report by Zhang and Ma [14], which showed that the rate and amount of apatite formation for a dense PLLA film were higher than those for a porous PLLA scaffold when soaked in a modified SBF.

Apatite formation on porous PLLA is greatly enhanced by addition of bioactive glass particles. After only 1 week of soaking in SBF, 9BG composites develop apatite both inside and on the surfaces (Fig. 7), while no apatite formed on PLLA or 29BG after 1 week. After 2 weeks of soaking in SBF, much more apatite forms inside and on both 9BG and 29BG composites as compared with porous PLLA alone. The delayed apatite formation rate for 29BG is due to its greater bioactive glass content, which results in more exposed glass surfaces and larger soaking ratio (defined as the ratio of the soaked glass surface area to the SBF volume). Previous research has demonstrated that an increase in soaking ratio results in a decrease in apatite development rate [52]. After the surfaces of 9BG composite are covered by apatite layers (Fig. 7), its inner microstructure remained almost unchanged between 1 and 2 weeks of soaking in SBF, likely due to the limited supply of SBF to the inside of the composites. Similar impeding effects for porous polysulfone/bioactive glass composites were demonstrated by Zhang et al. [12], and can be overcome by surface treatments that remove the denser outer layers.

Composites with silane pretreatment of bioactive glass particles formed less apatite compared with those containing non-treated glass. Compared with the apatite development for 9BG, the delayed apatite formation rate of 9BG/S may be related to the improved incorporation of BG in the PLLA matrix. With fewer glass surfaces exposed and the intervening layer of PLLA, the ion release rate from the bioactive glass particles is decreased. The slow ion release rate of hydroxyapatite particles coated by aminosilane was also reported by Dupraz et al. [37].

Previous research has correlated the ability of biomaterials to develop bone-like apatite upon soaking in SBF to bone bonding in vivo [44]. Therefore, the in vitro formation of bone-like apatite on porous PLLA/BG composites (with or without silane pretreatment) after soaking in SBF demonstrates their potential bone bonding ability. To assess the suitability of these materials for applications such as the interfaces attaching artificial cartilage to bone and GTR membranes, in vitro degradation studies and cell culture studies are the next step.

5. Conclusions

Porous poly(L-lactide)/bioactive glass composites were prepared by a phase separation technique. The composites are porous with an asymmetric structure consisting of a dense top layer and a porous substructure. The addition of bioactive glass enhanced the elastic modulus, but decreased the tensile strength and ductility of composites. The interface between PLLA and bioactive glass particles was improved by 3-aminopropyltrimethylsilane (APS) pretreatment of glass particles. Composites containing pretreated glass remained porous, but more glass particles were better incorporated into the PLLA matrix. The silane pretreatment enhanced the composites' mechanical properties in comparison with the composites containing non-treated glass. The potential bone bonding ability of the composites was demonstrated by the development of bone-like apatite inside and on the surfaces of the composites after soaking in SBF.

Acknowledgements

This work was supported primarily by the MRSEC program of the National Science Foundation under award numbers DMR-9809364 and DMR-0212302. We thank Dr. Hongwei Yan for his helpful discussion and Dr. David C. Bell for his help.

References

[1] Ambrosio AMA, Sahota JS, Khan Y, Laurencin CT. A novel amorphous calcium phosphate polymer ceramic for bone repair: I. synthesis and characterization. J Biomed Mater Res (Appl Biomater) 2001;58:295–301.

[2] Chen G, Ushida T, Tateishi T. Poly(DL-lactic-co-glycolic acid) sponge hybridized with collagen microsponges and deposited apatite particulates. J Biomed Mater Res 2001;57:8–14.
[3] Devin JE, Attawia M, Laurencin CT. Three-dimensional degradable porous polymer-ceramic matrices for use in bone repair. J Biomater Sci: Polym Edn 1996;7:661–9.
[4] Ignatius AA, Betz O, Augat P, Claes LE. In vivo investigations on composites made of resorbable cermics and poly(lactide) used as bone graft substitues. J Biomed Mater Res 2001;58:701–9.
[5] Kellomaki M, Niiranen H, Puumanen K, Ashammakhi N, Waris T, Tormala P. Bioabsorable scaffolds for guided bone regenration and generation. Biomaterials 2000;21:2495–505.
[6] Lee SJ, Park YJ, Park SN, Lee YM, Seol YJ, Ku Y, Chung CP. Molded porous poly(L-lactide) membranes for guided bone regeneration with enhanced effects by controlled growth factor release. J Biomed Mater Res 2001;55:295–303.
[7] Ma PX, Zhang R, Xiao G, Franceschi R. Engineering new bone tissue in vitro on highly porous poly(a-hydroxyl acids)/hydroxyapatite composite scaffolds. J Biomed Mater Res 2001;54: 284–93.
[8] Marra KG, Szer JW, Kumta PN, DiMilla PA, Weiss LE. In vitro analysis of biodegradable polymer blend/hydroxyapatite composites for bone tissue engineering. J Biomed Mater Res 1999;47: 324–35.
[9] Murphy WL, Kohn DH, Mooney DJ. Growth of continuous bonelike mineral within porous poly(lactide-*co*-glycolide) scaffolds in vitro. J Biomed Mater Res 2000;50:50–8.
[10] Qiu Q, Ducheyne P, Ayyaswamy PS. New bioactive, degradable composite microspheres as tissue engineering substrates. J Biomed Mater Res 2000;52:66–76.
[11] Walsh D, Furuzono T, Tanaka J. Preparation of porous composite implant materials by in situ polymerization of porous apatite containing ε-carprolactone or methyl methacarylate. Biomaterials 2001;22:1205–12.
[12] Zhang K, Ma Y, Francis LF. Porous polymer/bioactive glass composites for soft-to-hard tissue interfaces. J Biomed Mater Res 2002;61:551–63.
[13] Zhang R, Ma PX. Poly (a-hydroxyl acids)/hydroxyapatite porous composites for bone-tissue engineering. I. Preparation and morphology. J Biomed Mater Res 1999;44:446–55.
[14] Zhang R, Ma PX. Porous poly(L-lactic acid)/apatite composites created by biomimetic process. J Biomed Mater Res 1999;45: 285–93.
[15] Linhart W, Peters F, Lehmann W, Schwarz K, Schiling AF, Amling M, Rueger JM, Epple M. Biologically and chemically optimized composites of carbonated apatite and polyglycolide as bone subtitution materials. J Biomed Mater Res 2001;54:162–71.
[16] Zhang K, Grimm ME, Lu Q, Oegema TR, Francis LF. Porous composites for adhering artificial cartilage to bone. Materials Research Society Symposium Proceeding 2002;711:213–8.
[17] Bhardwaj T, Pilliar RM, Grynpas MD, Kandel RA. Effect of material geometry on cartilagenous tissue formation in vitro. J Biomed Mater Res 2001;57:190–9.
[18] Gao J, Dennis JE, Solchaga LA, Awadallah AS, Goldberg VM, Caplan AI. Tissue-enginnered fabrication of an osteochondral composite graft using rat bone marrow-derived mesenchymal stem cell. Tissue Engineering 2001;7:363–71.
[19] Ishikawa H, Koshino T, Takeuchi R, Saito T. Effects of collagen gel mixed with hydroxyapatite powder on interface between newly formed bone and grafted Achilles tendon in rabbit femoral bone tunnel. Biomaterials 2001;22:1689–94.
[20] Schaefer D, Martin I, Shastri P, Padera RF, Langer R, Freed LE, Vunjak-Novakovic G. In vitro generation of osteochondral composites. Biomaterials 2000;21:2599–606.
[21] Yaylanoglu MB, Yildiz C, Korkusuz F, Hasirci V. A novel osteochondral implant. Biomaterials 1999;20:1520–30.
[22] Niederauer GG, Slivka MA, Leatherbury NC, Korvick DL, Harroff Jr., HH, Ehler WC, Dunn CJ, Kieswetter K. Evaluation of multiphase implants for repair of focal osteochondral defects in goats. Biomaterials 2000;21:2561–71.
[23] Taboas JM, Maddox RD, Krebsbach PH, Hollister SJ. Indirect solid free form fabrication of local and global porous, biomimetic and composite 3D polymer-ceramic scaffolds. Biomaterials 2003;24:181–94.
[24] Agrawal CM, Ray RB. Biodegradable polymeric scaffolds for musculoskeletal tissue engineering. J Biomed Mater Res 2001; 55:141–50.
[25] Lu L, Mikos AG. The importance of new processing techniques in tissue engineering. MRS Bulletin 1996;21:28–32.
[26] Hench LL. Bioceramcis. J Am Ceram Soc 1998; 1705–1728.
[27] Loty C, Forest N, Boulekbache H, Kokubo T, Sautier JM. Behavior of fetal rat chondrocytes cultured on a bioactive glass-ceramic. J Biomed Mater Res 1997;37:137–49.
[28] Rich J, Jaakkola T, Tirri T, Nrhi T, Yli-Urpo A, Seppala J. In vitro evaluation of poly(ε-caprolactone-co-DL-lactide)/bioactive glass composites. Biomaterials 2002;23:2143–50.
[29] Marcolongo M, Ducheyne P, LaCourse WL. Surface reaction layer formation in vitro on a bioactiave glass fiber/polymeric composite. J Biomed Mater Res 1997;37:440–8.
[30] Wang M, Hench LL, Bonfield W. Bioglass/high density polyethylene composite for soft tissue applications: preparation and evaluation. J Biomed Mater Res 1998;42:577–86.
[31] Roether JA, Boccaccini AR, Hench LL, Maquet V, Gautier S, Jerome R. Development and in vitro characterisation of novel bioresorbable and bioactive composite materials based on polylactide foams and Bioglass for tissue engineering applications. Biomaterials 2002;23:3871–8.
[32] Stamboulis A, Boccaccini AR, Hench LL. Novel biodegradable polymer/bioactive glass composites for tissue engineering applications. Adv Eng Mater 2002;4:105–9.
[33] Liu Q, de Wijn JR, de Groot K, van Blitterswijk CA. Sufrace modification of nano-apatite by grafting organic polymer. Biomaterials 1998;19:1067–72.
[34] Orefice RL, Arnold JJ, Miller TM, Zamora MP, Brennan AB. Designed composite interfaces using novel polymeric coupling agents. Polym Prepr 1997;38:157–8.
[35] Androff NM, Francis LF, Velamakanni BV. Macroporous ceramics from ceramic-polymer dispersion methods. AIChE J 1997;43:2878–88.
[36] Drumright RE, Grumber PR, Henton DE. Polylactic acid technology. Adv Mater 2000;12:1841–6.
[37] Dupraz AMP, de Wijn Jr., VD, Meer SAT, de Groot K. Characterization of silane-treated hydroxyapatite powders for use as filler in biodegradable composites. J Biomed Mater Res 1996;30:231–8.
[38] Mohsen NM, Craig RG. Effect of silanation of fillers on their disperability by monomer systems. J Oral Rehab 1995;22:183–9.
[39] van de Witte P, Esselbrugge H, Peters AMP, Dijkstra PJ, Feijen J, Groenewegen RJJ, Smid J, Olijslager J, Schakenraad JM, Eenink MJD, Sam AP. Formation of porous membranes for drug delilvery systems. J Control Release 1993;24:61–78.
[40] Gibson LJ, Ashby MF. Cellular solids: structure and properties, 2nd ed. Cambridge, UK: Cambridge University Press; 1997. p. 120–68.
[41] Wang Y, Hillmyer MA. Polyethylene-Poly(L-lactide) diblock copolymers: synthesis and compatibilication of poly(L-lactide)/polyethylene blends. J Polym Sci: Part A 2001;39:2755–66.
[42] Ishai O, Cohen LJ. Elastic properties of filled and porous composites. Int J Mech Sci 1967;9:539–46.
[43] Kokubo T, Ito S, Shigematsu M, Sakka S, Yamamuro T. Mechanical properties of a new type of apatite-containing glass-ceramic for prosthetic application. J Mater Sci 1985;20:2001–4.

[44] Kokubo T, Kushitani H, Sakka S, Kitugi T, Yamanuro T. Solutions able to reporduce in vivo surface-structure changes in bioactive glass-ceramic A-W. J Biomed Mater Res 1990;24:721–34.
[45] Chiang CH, Ishida H, Koenig J. The structure of γ -aminopropyltriethoxysilane on glass surfaces. J Colloid Interface Sci 1980;74:396–404.
[46] Rehman I, Bonfield W. Characterization of hydroxyapatite and carbonated apatite by photo acoustic FTIR spectroscopy. J Mater Sci: Mater Med 1997;8:1–4.
[47] Pluedemann EP. Silane coupling agents. New York: Plenum Press; 1982. p. 115–51.
[48] Wijmans JG, Baaij JPB, Smolders CA. The mechanism of formation of microporous or skinned membranes produced by immersion precipitation. J Membrane Sci 1983;14:263–74.
[49] Bleach NC, Nazhat SN, Tanner KE, Kellomaki M, Tormala P. Effect of filler content on mechanical and dynamic mechanical properties of particulate biphasic calcium phosphate-polylactide composites. Biomaterials 2002;23:1579–85.
[50] Ferrigno TH. Principles of filler selection and use. In: Katz HS, Milewski JV, editors. Handbook of Fillers for plastics. New York: Van Nostrand Reinhold; 1987. p. 38.
[51] Brassell GW, Wischmann RS. Mechanical and thermal expansion properties of a particulate filled polymer. J Mater Sci 1974;9:307–14.
[52] Yan H, Zhang K, Blandford CF, Francis LF, Stein A. In vitro hydroxycarbonate apatite mineralization of CaO-SiO_2 sol-gel glasses with a 3-Dimensionally ordered macroporous Structure. Chem Mater 2001;13:1374–82.